

Potassium titanium hexacyanoferrate as a cathode material for potassium-ion batteries



Yushan Luo^{a,b}, Bolei Shen^{a,b}, Bingshu Guo^{a,b}, Linyu Hu^{a,b}, Qiuju Xu^{a,b}, Renming Zhan^{a,b}, Youquan Zhang^{a,b}, Shujuan Bao^{a,b}, Maowen Xu^{a,b,*}

^a Institute for Clean Energy & Advanced Materials, Southwest University, Beibei, Chongqing, 400715, PR China

^b Chongqing Key Laboratory for Advanced Materials & Technologies of Clean Energies, Beibei, Chongqing, 400715, PR China

ARTICLE INFO

Keywords:

Cathode
Nanoparticle
Potassium-ion battery
Prussian blue analogue

ABSTRACT

In this study, potassium titanium hexacyanoferrate ($K_{0.3}Ti_{0.75}Fe_{0.25}[Fe(CN)_6]_{0.95} \cdot 2.8H_2O$) was obtained by a simple co-precipitation and used as a cathode material in potassium-ion batteries (KIBs) for the first time. The reversible redox couples of Fe and Ti could provide $136.7 \text{ mA h g}^{-1}$ at 50 mA g^{-1} and 113 mA h g^{-1} at 100 mA g^{-1} in the first discharge. Considering that this material is easy to synthesize, with low cost and good electrochemical performance, our results suggest the possible development of KIBs as cathodes and future research into rechargeable KIBs.

1. Introduction

The consumption of energy has increased greatly due to the rapid economic growth of modern society. Secondary batteries are an energy storage method with increasingly important roles in energy conversion and energy storage. Lithium-ion batteries dominate the market for portable electronic devices, but the limited reserves and high price of lithium limit their application in large-scale energy storage systems [1,2]. Therefore, there is an extremely urgent need to find a new type of secondary battery. The alkaline metals sodium and potassium are more abundant compared with lithium and they have similar chemical properties. Sodium-ion batteries have been studied extensively but potassium-ion batteries (KIBs) are also attracting attention because of their unique advantages compared with sodium. First, the standard electrode potential of K (-2.93 V vs. the standard hydrogen electrode) is lower than that of Na (-2.71 V vs. the standard hydrogen electrode) [3]. Second, graphite can accommodate K de/intercalation reversibly and obtain a specific capacity of about 250 mA h g^{-1} in KIBs, whereas storage in Na is not possible [4]. Finally, K^+ has much weaker Lewis acidity than the other alkalis and it yields a smaller Stoke's radius for solvated ions, thereby leading to higher conductivity [5]. Thus, K electrolytes exhibit higher conductivity than Li and Na electrolytes [6]. Given these advantages, KIBs have rapidly attracted interest from researchers, and various materials have been developed and evaluated as potential KIB electrodes.

Several studies have reported progress with KIB anodes, including

carbonaceous materials [4,7], metals [8,9], metal oxides [10], and organic materials [11,12]. However, appropriate cathode materials need to be developed for KIBs. $K_xFe_2(CN)_6$ (PB) was reported by Eftekhari as a KIB cathode in 2004 [13], and PB and its analogues (PBAs) have been studied widely as low-cost cathode materials for use in batteries due to its high theoretical discharge capacity (156 mA h g^{-1}) and excellent electrochemical stability. The general chemical formula for PBAs is $A_xM[M'(CN)_6]_{1-y} \cdot nH_2O$ ($0 < x < 2$, $y < 1$), where A represents an alkaline metal ion or alkaline earth metal ion, M is a nitrogen-coordinated transition metal ions, and M' is a carbon-coordinated transition metal ions [14]. PBAs with different transition metal ions (Fe, Mn, Co, and Ni) have been reported and they exhibit advantageous performance as KIB cathodes in nonaqueous electrolytes. $K_{0.22}Fe[Fe(CN)_6]_{0.805} \cdot 4H_2O$ [15] with a vacancy-ridden and low potassium content has a capacity of 76.7 mA h g^{-1} with 50 mA g^{-1} and a low initial coulombic efficiency (CE) of 44.0%. Prussian white $K_{1.7}Fe[Fe(CN)_6]_{0.915}$ [16] with a high potassium content can provide a high capacity of 140 mA h g^{-1} and capacity retention of 60% after 300 cycles. PBAs exhibit good electrochemical performance, which indicates the feasibility of utilizing Prussian blue analogues as low-cost and high performance cathode materials for KIBs.

In this study, we synthesized a new class of PBA analogue, $K_{0.3}Ti_{0.75}Fe_{0.25}[Fe(CN)_6]_{0.95} \cdot 2.8H_2O$, called potassium titanium hexacyanoferrate (KTH) using a simple solution precipitation method. KTH with a face-centered cubic structure can provide a high reversible capacity of $136.7 \text{ mA h g}^{-1}$ at 50 mA g^{-1} and a first cycle CE of 118.86%.

* Corresponding author. Institute for Clean Energy & Advanced Materials, Southwest University, Beibei, Chongqing, 400715, PR China.
E-mail address: xumaowen@swu.edu.cn (M. Xu).

The results of this study provide insights into PBAs and they suggest that the Ti ion can be applied in KIB cathode materials.

2. Experimental

2.1. Synthesis of materials

All chemicals were analytical grade and used as received without further purification. In a typical procedure, The 0.03 M TiCl_3 solution was added dropwise to the $\text{KCl}/\text{K}_4\text{Fe}(\text{CN})_6$ (12 g KCl, 0.03 M $\text{K}_4\text{Fe}(\text{CN})_6 \cdot 10\text{H}_2\text{O}$) solution under magnetic stirring. The resulting solution was stirred continuously at 60 °C for 4 h and it changed color from orange to dark green. This solution was aged for 24 h at room temperature to obtain particles of uniform size. Next, the samples were separated by centrifugation, washed with deionized water and ethanol three times, and finally dried overnight at 60 °C in a vacuum oven.

2.2. Characterization of materials

The crystal structures of the products were recorded by powder X-ray diffraction (XRD, MAXima-X XRD-7000) with Cu K-alpha radiation ($\lambda = 1.5406$ nm) at a scan rate of 2° min^{-1} over a 2θ range from 10° to 80° . Furthermore, the morphologies and microstructures of the samples were examined by field-emission scanning electron microscopy (FESEM, JSM-7800F) and transmission electron microscopy (TEM, JEM-2100). X-ray photoelectron spectroscopy (XPS) measurements were obtained with a spectrometer (Escalab 250xi, Thermo Scientific). The molar ratio of the sample was analyzed by direct-reading inductively coupled plasma emission spectrometry (ICP-OES, Optima 8000). The moisture contents of the samples were determined by thermogravimetric analysis (TGA; TA Instruments, USA) and differential scanning calorimetry (DTA) at a heating rate of $10^\circ \text{ C min}^{-1}$ under N_2 flow from room temperature to 300 °C.

2.3. Electrochemical measurements

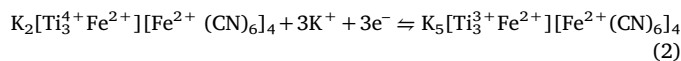
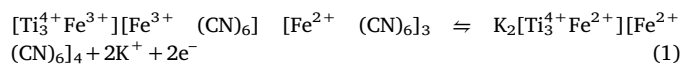
The working electrode was prepared by mixing the active material, super-P, and CMC binder (carboxymethylcellulose) at a weight ratio of 70:20:10 with distilled water to form a slurry. The well-mixed homogeneous mixture was coated on Al foil using a doctor blade and then dried at 60 °C in an oven for 24 h to remove the solvent. The typical loading of the material per electrode was approximately 1.0 mg. After drying, the working electrode was assembled in a half-cell configuration in 2032 coin cells. Potassium metal (Aladdin Ltd) pieces were used as the counter and reference electrodes, and Celgard 2400 was used as a separator. The electrolyte comprised 0.8 M KPF6 (99.5%, Aladdin Ltd) in ethylene carbonate:dimethyl carbonate ($v/v = 1:1$) with 5 wt% fluoroethylene carbonate additive (Sigma). The cells were constructed in an Ar-filled glove box and galvanostatic charge/discharge tests were then performed with a LAND cyler between 1.0 and 4.5 V (vs. K^+/K) at a desired current density using a Land battery testing system at room temperature. Cyclic voltammetry (CV) measurements were obtained at a scan rate of 0.2 mV s^{-1} by using an Arbin Instruments testing system.

3. Results and discussion

Fig. 1a schematically illustrates the framework for KTH built on an open three-dimensional (3D) framework comprising an MN_6 octahedron and $\text{M}'\text{C}_6$ octahedron ($\text{M} = \text{Fe}, \text{Ti}$). In the lattice of Prussian blue, two MN_6 octahedra were separated by one $\text{M}'\text{C}_6$ octahedron, and the MN_6 octahedron and $\text{M}'\text{C}_6$ octahedron were bridged together via a cyanide bond $-\text{C}\equiv\text{N}-$ to form a cubic open frame [17], which was expected to provide a channel for K ion de-intercalation. As shown in Fig. 1b, the positions of KTH and the relative intensities of all the diffraction peaks indexed perfectly to the PBs (JCPDS No. 52–1907), as shown by the characteristic peaks in the vicinity of $2\theta = 17^\circ, 25^\circ,$ and

35° [18]. There was a well-defined crystal structure with a face centered cubic structure in the $\text{Fm}\bar{3}\text{m}$ space group, which we suggest contained the structure of PB. The narrow diffraction peaks in the patterns indicated the high crystallinity of the as-prepared sample and the homogeneous distribution of the cations in the structure. XPS was employed to analyze the chemical composition and surface electronic state of the samples, which confirmed the chemical composition, as shown in Fig. S1. The survey spectrum indicated the presence of K (2s), Ti (2p), Fe (2p), C (1s), N (1s), and O (1s) elements. Fig. 2a and b shows the binding energies of Fe 2p and Ti 2p, respectively. The Fe 2p $_{3/2}$ and Fe 2p $_{1/2}$ peaks at 708.6 eV and 721.6 eV, respectively, with spin energy separation at 13.0 eV could be attributed to the presence of Fe^{2+} , and two binding energies with peaks located at 713.3 eV and 725.7 eV indicated the oxidation state of Fe^{3+} [19]. In addition, the binding energies of the Ti 2p $_{3/2}$ and Ti 2p $_{1/2}$ peaks were always at 464.1 eV and 458.4 eV, respectively (Fig. 2b) [20]. The morphology of KTH was examined by FESEM (Fig. 2c), which demonstrated that the size distribution of KTH was homogeneous, ranging from 50 nm to 80 nm. EDS mapping by FESEM indicated uniform distributions of K, Fe, Ti, C, and N (Fig. S2). TEM was used to further elucidate the structures and the high resolution TEM image (insets in Fig. 2d) indicated an inter-planar spacing of ~ 0.24 nm, which corresponded to the (420) plane of cubic PB. In addition, FESEM and TEM images of KTH at different magnifications are shown in Fig. S3. To further clarify the chemical composition of KTH, ICP-OES and EDS were used to determine the mass ratios of the elements, i.e., K, Ti, and Fe, as shown in Table S1. The precise chemical formula for the sample was calculated as $\text{K}_{0.3}\text{Ti}_{0.75}\text{Fe}_{0.25}[\text{Fe}(\text{CN})_6]_{0.95}$. Quantitative analysis of the water content of the KFH sample was conducted using TGA and DTA (Fig. S4) under an N_2 atmosphere. In the temperature range from 100 to 200 °C, the TGA results showed that the moisture content of the KTH sample was approximately 15.38 wt%, which corresponded to 2.8 H_2O molecules per formula unit. Therefore, the accurate chemical formula can be written as $\text{K}_{0.3}\text{Ti}_{0.75}\text{Fe}_{0.25}[\text{Fe}(\text{CN})_6]_{0.95} \cdot 2.8\text{H}_2\text{O}$.

The electrochemical performance of the as-prepared sample was investigated and the results are shown in Fig. 3. The CV curves were recorded for the KTH cathode at a scan rate of 0.2 mV s^{-1} in the voltage range from 1.0 to 4.5 V (vs. K/K^+), as shown in Fig. 3a. The electrode had an open-circuit voltage of 3.0 V and the CV behavior agreed with the following reactions.



The redox couple of $\text{Ti}^{3+}/\text{Ti}^{4+}$ was around 1.6/2.1 V and the Ti-ion was coordinated to nitrogen [21,22]. The $\text{Fe}^{2+}/\text{Fe}^{3+}$ redox couples were around 3.6/3.2 V and 4.3/3.7 V, where the former peaks from the redox reaction on the Fe site with a high-spin configuration coordinated to nitrogen, and the later peaks from the Fe site with a low-spin configuration coordinated to carbon [15,16]. Raman spectroscopy (Fig. S5) was also employed to determine the valence state of Fe because the frequency of the cyanide vibration stretching mode $\nu(\text{CN})$ is sensitive to the oxidation state of the coordinating iron. The $\nu(\text{CN})$ bands at 2138, 2108, and 2079 cm^{-1} indicated that Fe was in a bivalent state [23]. This result was consistent with the XPS spectra obtained for Fe (Fig. 2a). In subsequent scans, the anodic and cathodic peaks exhibited a narrower current response, which suggested an irreversible reaction at high potential in the earlier cycle and this was related to the formation of the solid electrolyte interphase (SEI) film. Subsequently, the peak current and polarization voltage increased gradually and the SEI film reached a complete and stable state [24]. The shapes of the peaks then remained almost unchanged during successive scans. In addition, the electrochemical impedance spectroscopy (EIS) spectrum was obtained to characterize the relationship between the SEI film and the electrode

Download English Version:

<https://daneshyari.com/en/article/7919817>

Download Persian Version:

<https://daneshyari.com/article/7919817>

[Daneshyari.com](https://daneshyari.com)